Invited Paper

# Advanced Virgo+ Status and future perspectives

Fabio Garufi[a,b]

[a]Dipartimento di Fisica 'Ettore Pancini' - Università degli Studi di Napoli 'Federico II', Complesso Universitario di Monte S. Angelo, Napoli, Italy
[b]INFN - Sezione di Napoli, Complesso Universitario di Monte S. Angelo, Napoli, Italy

## ABSTRACT

The Virgo detector contributed to the observations in the O3 observing run and increased its sensitivity from the initial 46 up to 60 Mpc during the run. The detector has undergone to a series of improvements since the end of the O3 observing run in view of O4, as the implementation of an additional recycling cavity at the output of the interferometer – the Signal Recycling cavity (SRC) – to broaden the sensitivity band, the Frequency Dependent Squeezing (FDS) to reduce quantum noise at all frequencies, and a new higher power laser.

Some criticality have emerged mainly due to the presence in Virgo of marginally stable recycling cavities with respect to the stable recycling cavities present in the LIGO detectors, which increases the difficulty in controlling the interferometer in presence of defects as those introduced by the high power on the mirrors. This resulted in a delayed joining the O4 run due to a longer than expected commissioning phase. At present the detector is running with a lower laser power (and a lower sensitivity w.r.t. the project design).

A new stop of about 2 yr is planned between O4 and O5 starting in 2027, to implement new upgrades (phase II). To improve the stability of the interferometer, we are considering a large upgrade to introduce stable cavities and this will imply heavy infrastructural works also with the minimal design. The aim is to reach a Binary Neutron Star (BNS) sensitivity larger than 100 Mpc.

Plans are being made for the post-O5 period as a bridge between 2nd and 3rd generation detectors and a new collaborative effort has born under the name of Virgo_nEXT with the aim to keep and push the infrastructure and maintain alive the community.

**Keywords:** Gravitational Waves, Interferometer, GW astronomy

## 1. INTRODUCTION

The Virgo Collaboration counts more than 897 Members representing 153 Institutions in 17 different countries (as for May 2024). It maintains and runs the Virgo interferometer for the detection of Gravitational Waves (GW), and is part of the LIGO-Virgo-Kagra (LVK) collaboration. Within the LVK, data exchange and data analysis are pursued as a single observatory with 4 instruments (2 LIGOs in U.S.A., Virgo in Italy, and Kagra in Japan).

Virgo is hosted by the European Gravitational Observatory (EGO) – a consortium founded by the French CNRS and Italian INFN – in the flooding plane of the Arno river in Cascina in the province of Pisa. After several observation runs starting from 2007, without detection, the interferometer was shut down in 2011 to allow for significant upgrades as part of the Advanced Virgo (AdV) project[1] entered in operation within the Network of GW detectors in 2017 with the second Observation Run – O2, just in time to concur to the localization of the exceptional event GW170817,[2] the first, and at present only, event observed with GW and the whole electromagnetic spectrum.

Further author information: (On behalf of the Virgo collaboration).
Send correspondence to Fabio Garufi: E-mail: fabio.garufi@na.infn.it, Telephone: +39 081 676 457

Ground-based and Airborne Telescopes X, edited by Heather K. Marshall,
Jason Spyromilio, Tomonori Usuda, Proc. of SPIE Vol. 13094, 130941C

doi: 10.1117/12.3028936

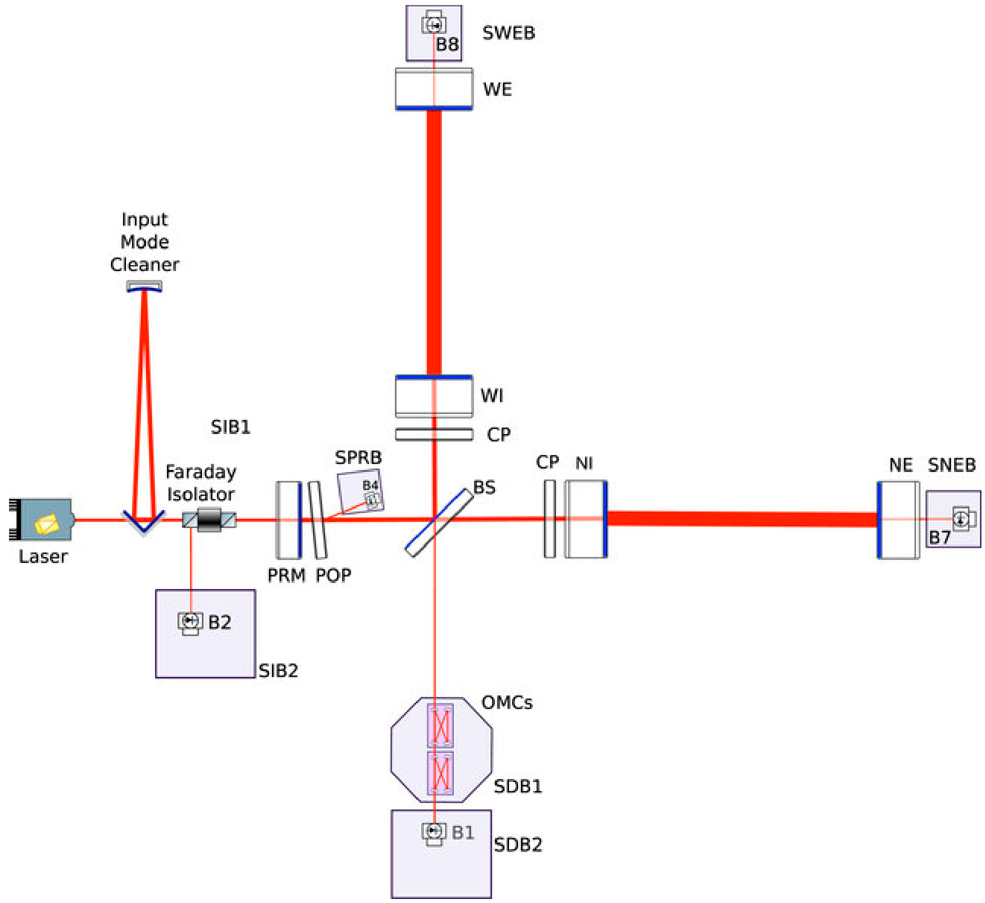


Figure 1. Schematics of the AdV configuration during the O3 run (not to scale) showing the optics as from.[4] The main abbreviations labelled on the schematic are explained in the main text.

## 2. ADVANCED VIRGO DURING THE THIRD OBSERVATIONAL RUN O3

The third observation period of the Network of Gravitational Waves interferometeric detectors –O3 – ended on march 2020. Despite the lower sensitivity w.r.t. the LIGO detectors, Virgo contributed to the observation of many exceptional events,[3] e.g.: GW191219_163120, an extremely unequal masses NS-BH coalescence and the lightest NS ever observed, or BH-BH coalescences with very high massess

The AdV detector during O3, is configured as a power-recycled Michelson Interferometer with Fabry-Perot cavities in the 3 km long arms. The simplified optical schematic of AdV during the O2 and O3 runs is shown in Figure 1. In the following, we briefly outline the different parts of the detector layout and define the main abbreviations that are labelled on the schematic or used later in the article.

The Virgo power-stabilized laser beam (PSL, wavelength: 1.064 $\mu$m) is filtered at the interferometer input by a 144 m long triangular cavity called the Input Mode Cleaner (IMC) the two flat mirrors of the IMC are located on the first suspended injection bench (SIB1), that also hosts various optics for beam matching. Then, the beam goes through the partially reflective Power Recycling (PR) mirror before being split into two perpendicular beams at the Beam Splitter (BS) mirror. The two 3 km-long arms hosting Fabry-Perot cavities are called ”North” and ”West” as they are roughly oriented along these geographical directions. In these cavity, the closest mirror to BS is called the ”input” mirror, the farthest is the ”end” mirror, at the end of the 3 km arm. So, following these conventions, the test masses (the four mirrors forming the two 3-km long Fabry-Perot cavities) are labelled NI, NE, WI and WE. Both arms end with a suspended terminal bench –called SNEB or SWEB – hosting a photodiode (B7 or B8) receiving the cavity transmitted beam. After propagation and phase accumulation (and power build-up) in the kilometric cavities, the arm beams recombine on the BS and the beam resulting from this

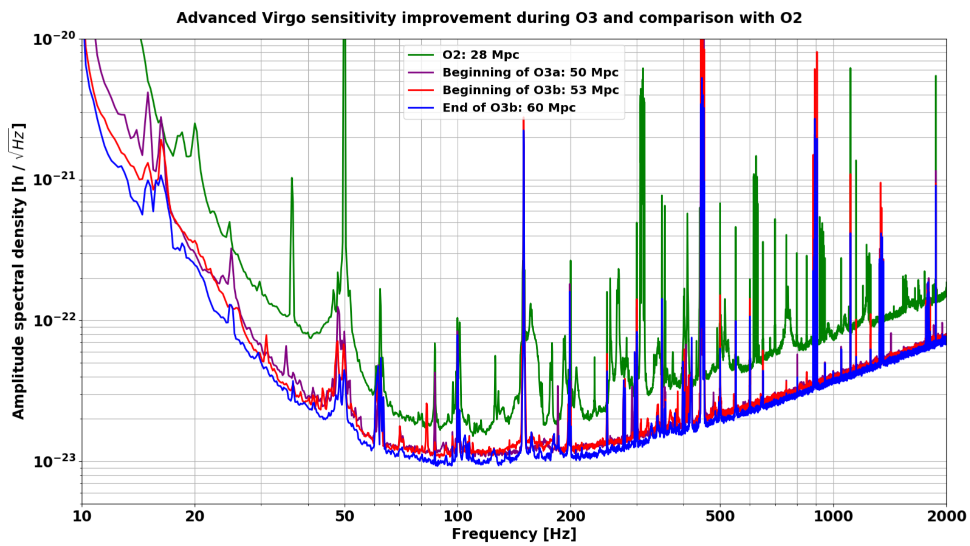


Figure 2. Evolution of AdV sensitivity curve during O3 and comparison with O2. The corresponding BNS range is in the legend

interference goes to the interferometer output port where two suspended detection benches (SDB1 and 2) host the Output Mode Cleaners (OMCs) and the detection photodiode(s).

The light returning back towards the laser is recycled into the inteferometer by means of the Power Recycling Mirror (PRM), and the power in in the cavity is monitored by the photodiode placed on the PR suspended bench (SPRB) reading the light reflected by the Pick-Off Plate (POP) placed downstream the PRM. The residual light transmitted by PRM is blocked before reaching the PSL by means of a Faraday isolator.

The global interferometer control relies on radio-frequency sidebands for the carrier beam that are generated by the electro-optical modulator (EOM - not shown in figure) located in between the laser source and the IMC.

To compensate thermal effects on the mirrors' radius of curvature (RoC), a thermal compensation system based on ring heaters around the mirrors and $CO_2$ lasers projected on the compensation plates (see Fig 1) in front of the Input Masses, has been installed since O2. Moreover, to beat the fundamental limit due to the shot noise at high frequency, a beam of Frequency Independent squeezed (FIS) light is injected at the output port (virtually at the expenses of sensitivity at 20-50 Hz due to increased radiation pressure, that has not been truly a limit due to sources of higher noise). With this configuration the detector, during O3 improved its sensitivity from 50 to 60 Mpc, expressed as the maximal distance a $1.4 + 1.4 M_\odot$ Binary Neutron Star (BNS) coalescence is visible with a Signal to Noise Ratio SNR=8.

## 3. THE O4 DESIGN CONFIGURATION

The optical configuration of the AdV+ interferometer initially foreseen for the so called Phase I is shown in Figure 3.

In synthesis the improvements foreseen before entering O4 are:[5]

1. Higher power Laser amplifier.
2. Signal recycling mirror on the anti-symmetric port.
3. Frequency dependent squeezing (FDS) to beat Shot noise at high frequency and radiation pressure at the low frequency end.
4. Green light auxiliary laser to control the arm cavities independently w.r.t the central area degrees of freedom.

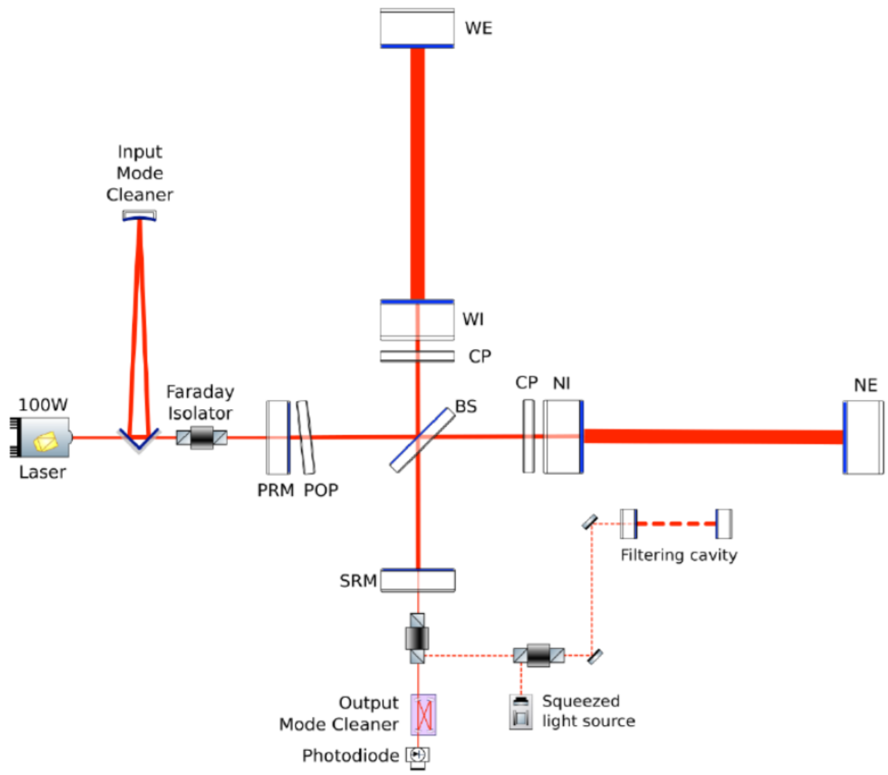


Figure 3. The design interferometer configuration for O4 as from[5]

5. Scattered light mitigation
6. New Input mode Cleaner payload with an instrumented baffle to monitor and cut stray light.
7. New high finesse output mode cleaner and new read-out photodiodes.
8. High vacuum upgrades and reduction of environmental noise.
9. Deployment of accelerometer arrays for Newtonian Noise characterization

The intended sensitivity downstream those installations correspond to a BNS range of 90-115 Mpc; Not all the foreseen modifications, however, resulted in the intended improvement of the detector performances. In the following we will go through the list of changes and discuss the problems found and the solutions adopted that allowed the detector to enter O4 in the second half with reduced performances w.r.t. the design.

### 3.1 The Laser source

Given the ageing of the NeoVan Power Stabilised Laser and a failure of its slave laser, it was replaced with a new laser with a fibre amplifier. This solution, however, proved to be noisier than the original, so, at the end we reinstalled the old Neovan equipped with a new slave laser.

As we will see in the following, the increase of input power (from 25W to 33W, however less than the 40 W design power) improves the shot noise, but leads to higher radiation pressure effects (affecting the control of the detector) and other, even stronger, thermal effects (affecting both the control and the optical performance of the detector). Despite the operation of an active thermal compensation system (see section 3.3), the detector resulted rather unstable with the higher power and even the introduction of a correction of the radius of curvature was not enough to operate a stable interferometer. The input power has, thus, gradually been reduced to the present 18W.

### 3.2 Signal Recycling cavity

The Signal recycling mirror at the dark port, enhances the detector sensitivity and introduces a new cavity to be controlled both in angular and longitudinal degrees of freedom. Also the lock acquisition procedure has to be re-designed to take into account the locking of this new coupled cavity.

The implementation of the signal recycling technique requires auxiliary green lasers to control the 3 km arm cavities independently of the rest of the interferometer. This allows to add a common offset to the arms, bringing the main laser source out of resonance, avoiding main IR laser power build-up in the cavities.

The introduction of recycling mirrors, as said above, configures two resonating cavities: the power recycling cavity (PRC) and the signal recycling cavity (SRC). The second mirror of these cavities is the so called compound, i.e. the 'central' interferometer (CITF). So the SRC (see Figure 3) cavity length, for example is: $SRCL = l_S + \frac{l_W + l_N}{2}$, where $l_S$ is the SRM-BS distance and $l_{N,W}$ are the BS-[N,W]I mirrors. After the central area d.o.f. are controlled, the offset on the common mode is then gradually reduced, so that thermal effects due to power increase can be controlled near the lock point.

For Gaussian beams, as is the case of our detectors, the cavity is stable if a paraxial ray is focused inside the cavity (i.e. the beam waist position is inside the cavity) after an arbitrary number of reflections. The stability is linked to mirrors' Radius of Curvature (RoC), $R$, and distance $L$ by means of the Guoy phase $\phi = arccos(\sqrt{g_1 g_2})$ where $g_i = 1 - \frac{L}{R_i}$. The cavity is stable when $0 < g_1 g_2 < 1$, i,e $-\pi/2 < \phi < \pi/2$. In a stable cavity, the Gaussian modes of the beam are not degenerate, i.e. only one resonate (TEM00 for us), while all the higher order modes don't.

When the AdV Project was started, the implementation of a stable cavity would have required heavy infrastructural works, thus, to enter in time in O2 and remain into the available budget, a marginally stable cavity – i.e. $g_1 g_2 \simeq 0.9999981$ – was implemented.

### 3.3 The thermal compensation system

While building a marginally stable Power recycling cavity (MSPRC) has paid off, allowing the participation to the discoveries of O3, it resulted in a hypersensitivity to mirror defects (errors on Radius of Curvature, absorption points, optical aberrations, induced by cold and hot defects), to cavities mode matching and alignment and so a major source of difficulties during the commissioning phase. The main problem is that the Power Recycling mirror has a pre-tuned RoC, to be compliant with the 125W design input power, which makes the cavity unstable for lower powers. To overcome this last issue, an additional actuator – Central Heating Radius of Curvature Correction (CHRoCC) – has been installed to re-tune the PRM RoC and stabilize MSPRC, while a ring heater is used to tune the SRM.

To ease the locking, auxiliary green laser beams are used to control the arm cavities independently of the central interferometer (CITF). In this way, the main laser can be kept not resonant in the arms until the CITF is controlled, then resonance can be gradually restored so that thermal effects due to power build-up can be controlled near the lock point.

When we started the commissioning toward O4 with a power of 40W and then 33W, the introduction of CHRoCC improved the lock stability but not enough, so we were compelled to lower the input power, and then raise again step by step, stopping at the present 18W.

### 3.4 Injection of frequency dependent squeezed vacuum states

The injection of frequency dependent squeezed light, allows to reduce shot noise at high frequencies and radiation pressure noise at low frequencies. Actually, since the light is injected at the dark port, the injection is made with squeezed vacuum states. The squeezed light source by AEI is the same used for frequency independent squeezing during O3,[6] the difference now is that the injected squeezed states are phase squeezed at high frequency, where the shot noise is dominant, and amplitude squeezed at low frequency, where radiation pressure has to be damped.[7] To this end, a 300m long high finesse filter cavity has been built for rotating the squeezing ellipse below 50 Hz. High-throughput Faraday insulators and beam optics are suspended under vacuum for stray-light mitigation.

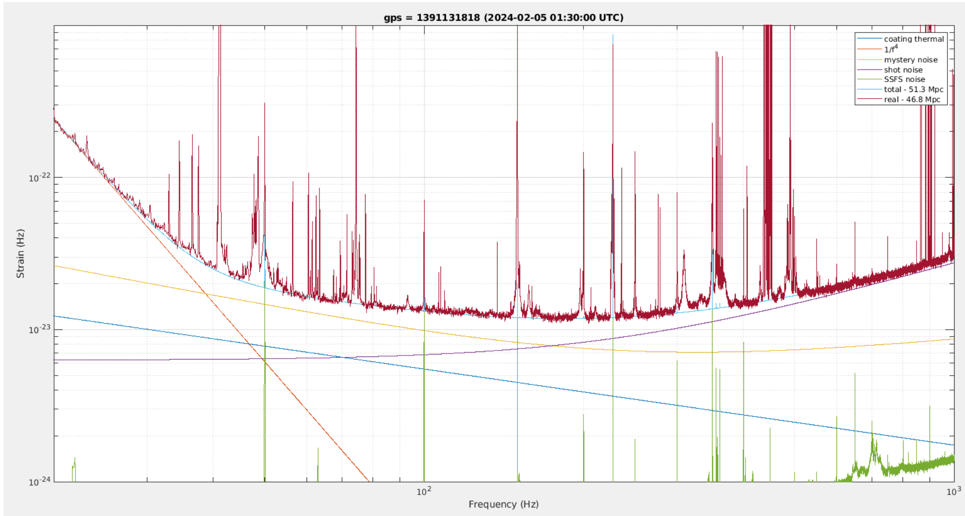


Figure 4. The sensitivity curve just before O4 is mostly explained by the sum of known sources of noise as shot noise at high frequency and coating and control noise at low frequencies. To explain the curve between 40 and 200 Hz, a $1/f^{2/3}$ "mystery noise" must be considered dominating in this range

### 3.5 Other add-ons for O4

An instrumented baffle has been installed to block stray light and, at the same time, get information on its provenience in the IMC. Although passive baffles were already installed and served their purpose, absorbing 99.5% of the Stray Light (SL), there is no real control or monitoring of where the SL goes or comes from. Virgo main arms do not have active sensors in the vicinity of the test masses to assist in the pre-alignment of the interferometer. The instrumented baffles implement 76 photosensors behind the absorbing plate mounted on a large PCB. Stray Light reach the sensors through 12° conical holes in the plate to avoid back-reflection. Data transmission is via wi-fi.

Arrays of accelerometers and microphones and a prototype tilt meter have been installed near the main suspensions to characterize Newtonian noise.

Profiting of a shut down due to the replacement of a broken fibre in a suspension, some other intervention have been carried-out as e.g. fixing a wobbly magnet on a payload.

### 3.6 AdV+ Entering in O4

On March 20 2024, Virgo started the Engineering run preparatory to O4b with a average BNS initial range of about 52 and a input power of 18W and then, on April 10, entered in O4b with a sensitivity around 55 Mpc.

Technical noise and a misalignment of the signal recycling cavity, necessary to move the pole of the SRC to lower frequency and gain in sensitivity in the BNS range, restricted the implementation to FIS during O4b. This circumstance, however, does not spoil the sensitivity at low frequency, that is dominated by other sources of noise as we will see in the following, while FIS accounts for a few Mpc gained in sensitivity at high frequencies. Nevertheless, Virgo extensively tested and commissioned the FDS system in standalone mode with a homodyne detector.[7] Commissioning activity is always in course during the Tuesdays maintenance break to improve sensitivity and understand e.g. the so called "mystery noise", i.e. a $1/f^{2/3}$ noise spoiling sensitivity below 200 Hz (see simplified LF noise budget in Figure 4), that seems to be the main responsible for the missing Mpc in BNS horizon, and whose cause has not yet been identified.

## 4. PHASE II COMMISSIONING AFTER O4

Phase II commissioning is intended to be exploited in the period between O4 and O5. Since 2019 when Phase II was originally presented, several (new) factors have entered the horizon that have pushed for a review of the baseline design for O5.

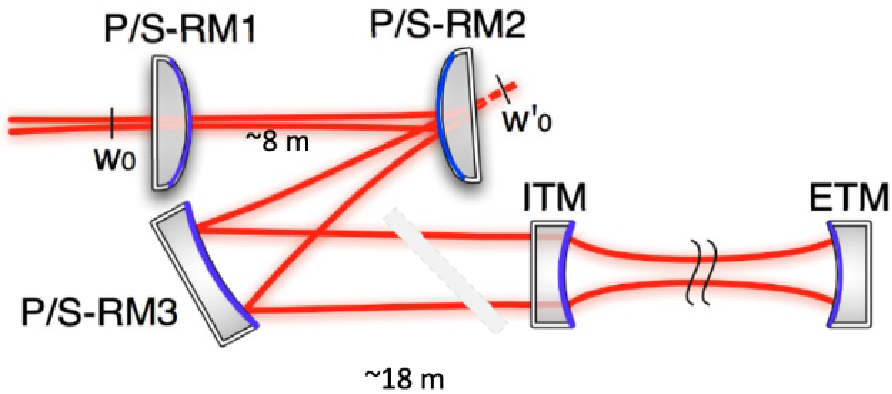


Figure 5. The stable recycling cavity optical design

Given the difficulties in operating with MSRC, priority will be given to the implementation of stable recycling cavities. After a detailed study, a short (folded $\approx 35m$) cavity was chosen, similar to LIGO's (see Figure 5) that would touch less heavily the infrastructure than other options, but needs two benches at both the input port and the output port, removal of 2 large vacuum chambers and addition of 8 smaller vacuum chambers. It also needs to suspend the signal recycling and power recycling mirror on the top of suspended benches that are still at the level of conceptual design an will require the development of a prototype. Some constrains are also imposed by the control strategy on how sidebands resonate in recycled cavities and in the arms.

### 4.1 O5 configuration

Given these premises, as said above, some of the original Phase II improvements, e.g. large beams and large mirrors are delayed after implementation and running with the stable cavities. Upgrades for High Order Modes (HOMs) mitigation are planned such as: replace test masses with point-absorber-free ones and develop a procedure to avoid point absorbers due to contamination during installation. The new test masses will be obtained by re-polishing substrates purchased for AdV+ Phase II. A new laser amplifier is also needed, because the present laser cannot provide more than 30W, and several other upgrades on injection optics and environmental noise cancellation will also be implemented. A new generation of DSP cards will be (is being) developed to replace the present one due to component obsolescence and lack of spares.

After all the above mentioned upgrades and other now being discussed, the goal is to have for O5 a sensitivity (BNS range) above 100 Mpc, provided mystery noise is canceled.

## 5. VIRGO_NEXT

What about Virgo after O5? To keep the community united, continue observations, not waste the acquired instrument knowledge and exploit the R&D on technologies to be used in 3rd generation detectors in the period between the end of O5 (2028-29) and the entrance in operation of the 3rd generation interferometers (Einstein Telescope and Cosmic Explorer $->$ 2035), the "Virgo_nEXT"[8] project has been conceived.

The Virgo_nEXT concept study was presented to the Science and Technology Advisory Committee (STAC) in May 2022 and to the Council in June 2022.

The baseline configuration for Virgo_nEXT is the initial O5 configuration, with more power injected and stored in the cavities, larger beams and heavier mirrors, suspended through an intermediate additional suspension stage, and finally a new design for output mode cleaner cavities.

After the rescoping of AdV+ phase II, the Virgo_nEXT project will undergo to unavoidable changes, presently being discussed.

## REFERENCES

[1] Acernese, F. et al., "Advanced virgo: a second-generation interferometric gravitational wave detector," *Classical and Quantum Gravity* **32**, 024001 (dec 2014).

[2] Abbott, B. P. et al., "GW170817: Observation of Gravitational Waves from a Binary Neutron Star Inspiral," *Phys. Rev. Lett.* **119**, 161101 (Oct 2017).

[3] Abbott, R. et al., "GWTC-3: Compact Binary Coalescences Observed by LIGO and Virgo during the Second Part of the Third Observing Run," *Phys. Rev. X* **13**, 041039 (Dec 2023).

[4] M W a., Gouaty, R., and Bonnand, R., "End benches scattered light modelling and subtraction in advanced virgo," *Classical and Quantum Gravity* **38**, 075020 (mar 2021).

[5] Acernese, F. et al., "Advanced Virgo Plus Phase I Design Report," Virgo note VIR-0596A-19, The Virgo Collaboration (2019).

[6] Acernese, F. et al., "Increasing the Astrophysical Reach of the Advanced Virgo Detector via the Application of Squeezed Vacuum States of Light," *Phys. Rev. Lett.* **123**, 231108 (Dec 2019).

[7] Acernese, F. et al., "Frequency-Dependent Squeezed Vacuum Source for the Advanced Virgo Gravitational-Wave Detector," *Phys. Rev. Lett.* **131**, 041403 (Jul 2023).

[8] Arnaud, N. et al., "Virgo next: beyond the adv+ project. a concept study," Virgo note VIR-0497A-22, The Virgo Collaboration (2022).